Dynamic Cervical Vertebral Motion of Female and Male Volunteers and Analysis of its Interaction with Head/Neck/Torso Behavior during Low-Speed Rear Impact

Fusako Sato, Taichi Nakajima, Koshiro Ono, Mats Svensson, Karin Brolin, Koji Kaneoka

Abstract The purpose of this study was to clarify the characteristics of dynamic head/neck/torso and cervical vertebral motion for females and males in a rear impact by reanalyzing two series of rear impact sled tests. One was a test series with 12 males and 8 females, the latter not previously published. Whole body visual motion was measured by a high speed video camera. The second series was conducted with 4 males and 2 females. Cervical vertebral motion was measured by cineradiography, as well as visual motion through a high-speed video camera. The general characteristics of female visual motions were derived from the two test series. Cervical vertebral motion was then investigated.

The females had a peak flexion of the head relative to neck link, defined as a line between T1 and the occipital condyle, while the neck link was extension at the time of peak head flexion. On the other hand, the males had flexion in both the head relative to neck link and neck link relative to T1 up to 100ms. Likewise, the females had larger flexion in the upper vertebral segments and larger extension in lower vertebral segments, when analysing the cervical spine motion. The cineradiography data showed the same tendency as that of the overall neck motion and supported that the head relative to neck link and neck link relative to T1 indicated S-shape deformation of the neck.

Keywords Whiplash, Rear Impacts, Volunteers, Neck, Cervical vertebral motion

I. INTRODUCTION

Whiplash associated disorder (WAD) is a worldwide problem. WAD is more often caused by rear impacts than by any other type of automobile impacts [1-2]. Preventive measures for WAD in rear impacts have been installed in car seats, and advanced seats with concepts for whiplash protection have been introduced since the late 1990s. Kullgren [3-4] reported that those types of seats have reduced the risk of WAD and proved to be more effective for males than females. The susceptibility of females to WAD has been the focus of many previous studies, showing that females have a higher risk of sustaining WAD than males. Carlsson [5] summarized those studies and reported that the relative injury risk was approximately 1.5 to 3 times higher for females compared to males in rear impacts. Harder [6] reported that gender is a statistically significant factor and that females tend to have a longer recovery after sustaining a WAD. Therefore, further research to understand the injury biomechanics and prevent WAD more effectively is needed for females as well as males.

Dynamic response of occupants in rear impacts has been analyzed by conducting volunteer tests in order to understand the biomechanics of WAD. Linder [7] and Carlsson [5] reanalyzed data published by Siegmund [8] and revealed gender differences in the kinematic response, acceleration and overall neck motion for volunteers in sled tests. However, detailed data on the kinematics of individual spinal segments are lacking. Stemper [9] conducted rear impact sled tests with post mortem human head-neck complexes instrumented with retro-reflective targets inserted in each vertebra. The study found that during impact the cervical intervertebral angles were significantly greater for the female specimens than for the male specimens. A few studies have used the approach to investigate cervical vertebral kinematics of volunteers using a cineradiography system [10-14]. In one of these studies, Ono [13] conducted rear impact sled tests with both female and male volunteers and showed that the females had larger intervertebral angles compared to the males. The study mainly focused on strain at the facet joint capsules and did not analyze vertebral kinematics in great detail.

The goal of this study was to clarify the characteristics of dynamic head/neck/torso behavior and cervical

F. Sato is a researcher at the Japan Automobile Research Institute (JARI) (tel: +81-29-856-0885, fsatou@jari.or.jp). T. Nakajima is a researcher at JARI. K. Ono is the Executive Research Adviser & Research Director at JARI. M. Svensson is Professor and K. Brolin is Associate Professor in Impact Biomechanics at Chalmers University. K. Kaneoka is medical doctor and Professor in faculty of sport sciences at Waseda University.

vertebral motion responses for both female and male volunteers in rear impact tests. This was done by reanalyzing the data obtained by Ono [13] in order to determine the female and male characteristics in terms of overall neck and individual cervical vertebral kinematics.

II. METHODS

Two series of rear impact sled tests with volunteers were used. One is data from an incline-sled test series with a total of 12 males which are presented in Ono [11-12], and with an additional 8 females that has not previously been published (Test Series 1). Whole body kinematics was measured by a high-speed video camera. The second set of data is from a mini-sled test series with 4 males and 2 females by Ono [13] (Test Series 2). Cervical vertebral kinematics was measured by a cineradiography system, as well as whole body kinematics through a high-speed video camera. The consent of the volunteers was obtained before testing commenced. The test protocol was subjected to the approval of the Special Committee of Ethics, Medical Department, University of Tsukuba.

In this study, the time histories of the whole body and cervical vertebral kinematics were reanalyzed in order to specify the characteristics of the female kinematic response during rear impacts. Peak values, and their timing and interaction between overall neck and cervical vertebral kinematics were investigated as further analysis. In addition, those response corridors were generated for females and males.

Test Procedures -Test Series 1

Fig. 1 shows a schematic view of the incline-sled apparatus. A rigid seat, with a seatback angled 20° from the vertical, was mounted to a sled, and the sled was set on 4m incline rails angled 10° from the horizontal line. The rear-end impact was simulated by releasing the sled from the top of the rails. A hydraulic damper was used on the posterior part of the rails to decelerate the sled. Two sled decelerations were used. The time history of the sled accelerations and velocities are presented in Fig. 2. The Δ V and peak acceleration were 8.1 km/h and 27 m/s^2, respectively, with impact velocity of 6.2 km/h for sled pulse 1 and 10 km/h and 37 m/s^2, respectively, with impact velocity of 7.9 km/h for sled pulse 2.

Volunteers were seated on the rigid seat and asked to relax. Two biaxial accelerometers were mounted on the head rig shown as a green bar in Fig 1 to obtain the head c.g. acceleration. The head rig was fastened to the forehead and mouth via a mouthpiece. For T1 acceleration, a biaxial accelerometer was mounted on the skin surface of the T1 process. Target markers were applied at the auditory canal, the skin surface of the T1 process and upper sternum, and iliac crest for video tracking of the motion with a high-speed video camera at 500 fps. The age and physical data of volunteers are shown in Table I.

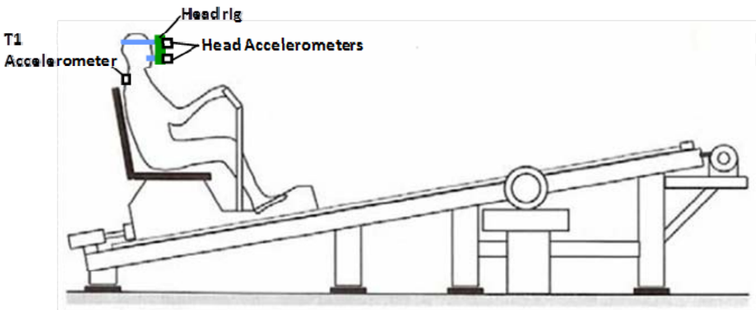

Fig. 1. Scheme of test series 1

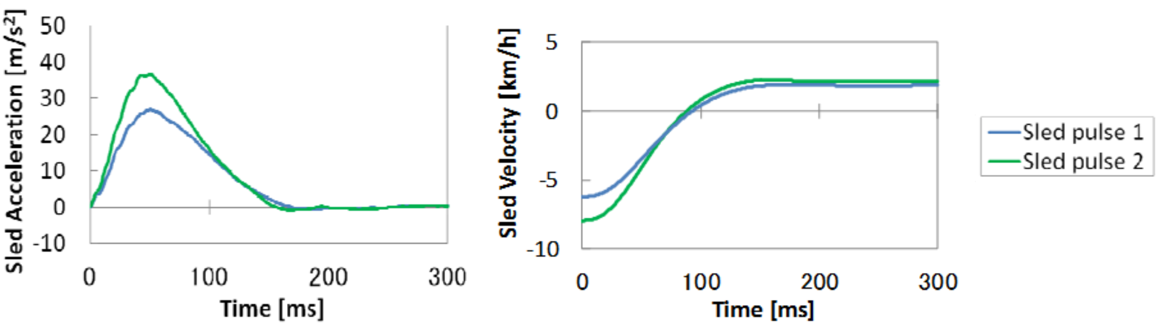

Fig. 2. Time history of the sled accelerations and velocities, test series 1

TABLE I DETAILS OF THE VOLUNTEERS IN TEST SERIES 1

(a) Female

ID	Tests	Sex	Age [year]	Height [cm]	Weight [kg]
F-I	Sled pulse 1&2	F	23	166	51
F-II	Sled pulse 1&2	F	22	154	53
F-III	Sled pulse 1&2	F	22	162	46
F-IV	Sled pulse 1	F	21	150	42
F-V	Sled pulse 1	F	22	163	54
F-VI	Sled pulse 1	F	23	163	48
FVII	Sled pulse 1	F	24	158	51
F-VIII	Sled pulse 1	F	22	152	55

(b) Male

ID	Tests	Sex	Age [year]	Height [cm]	Weight [kg]
M-I	Sled pulse 1&2	M	22	175	73
M-II	Sled pulse 1&2	M	23	174	71
M-III	Sled pulse 1	M	34	176	72
M-IV	Sled pulse 1&2	M	25	181	79
M-V	Sled pulse 1&2	M	24	173	65
M-VI	Sled pulse 1&2	M	23	178	73
M-VII	Sled pulse 1&2	M	33	174	66
M-VIII	Sled pulse 1&2	M	24	174	71
M-IX	Sled pulse 1	M	25	176	79
M-X	Sled pulse 1&2	M	22	174	70
M-XI	Sled pulse 1&2	M	21	171	69
M-XII	Sled pulse 1&2	M	22	172	61

Test Procedures -Test Series 2

Fig. 3 shows a schematic view of the mini-sled apparatus. A rigid seat, with a seatback angled 20° from the vertical, was mounted to a sled. The sled was set on 2m horizontal rails and accelerated by release of a compressed spring installed on the end of the sled. A hydraulic damper was used on the anterior part of the rails to decelerate the sled. Fig. 4 shows the time history of the sled acceleration and velocity. The Δ V was 5.8 km/h and the peak acceleration was 42 m/s^2.

Volunteers were seated on the rigid seat and asked to relax. A 3-axis accelerometer and a 3-axis angular velocimeter were mounted on the mouth via a mouthpiece and the skin surface of the T1 process to obtain the head and T1 accelerations. Target markers were applied at the auditory canal, the skin surface of the T1 process and sternum, and trochanter to video track motion with a high-speed video camera at 500 fps. The cervical vertebral kinematics was captured at 60 fps by a cineradiography system (Integris Allura BH-5000, Philips Medical System) at the University of Tsukuba Hospital. The age and physical data of volunteers are shown in Table II.

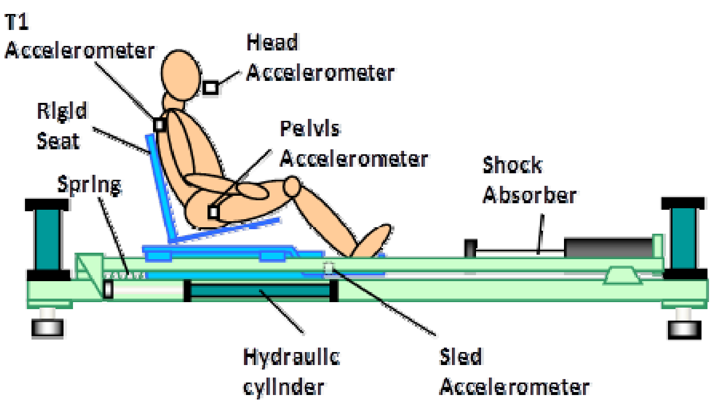

Fig. 3. Scheme of test series 2

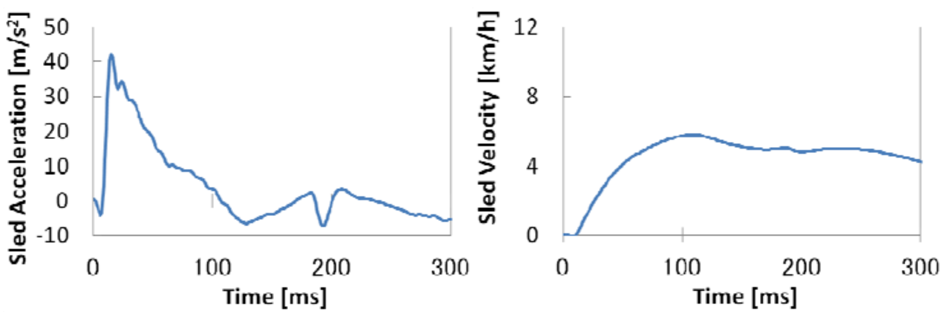

Fig. 4. Time history of the sled acceleration and velocity, test series 2

TABLE II DETAILS OF THE VOLUNTEERS IN TEST SERIES 2

ID	Sex	Age [year]	Height [cm]	Weight [kg]	Initial C7 angle [deg]
I	F	23	164	50	-7
II	F	23	162	46	-4
III	M	23	176	67	-16
IV	M	25	166	61	-10
V	M	25	171	57	-25
VI	M	24	178	67	-19

Definitions of Five Local Coordinate Systems

Five local orthonormal coordinate systems were defined to analyze head, neck and torso kinematics during impact. In all local coordinate systems, the positive direction is extension and negative flexion.

Sled coordinate system: Its x-axis is horizontal and positive forward, the y-axis horizontal and positive to the right, and the z-axis vertical and positive downward. The coordinate system moves with the sled.

Head anatomical coordinate system: Fig. 5 (a) shows the head anatomical coordinate system. The origin was defined at the anatomical centre of gravity of the head [15], located at a point which was 5mm anterior of the auditory canal on the Frankfurt line and superiorly 20mm perpendicular to this line. Its x-axis is parallel to the Frankfurt line and positive forward, and z-axis positive downward.

T1 accelerometer coordinate system: Fig. 5 (b) shows the T1 accelerometer coordinate system. Its z-axis is along the the skin surface of the T1 process and positive downward, and x-axis positive forward.

T1 anatomical coordinate system: Fig. 5 (c) shows the T1 anatomical coordinate system. The origin was defined at the center of T1, which was estimated at the midpoint between the T1 and sternum skin markers. Its z-axis is along a line through the occipital condyle at the initial posture and positive downward. The x-axis is positive forward. The coordinate system moves with the T1-Sternum line represented as a red line in Fig. 5 (c).

Lower vertebral coordinate system: Fig. 5 (d) shows the lower vertebral coordinate system. The origin was defined at the most inferior and posterior point of the lower vertebral body. Its x-axis is along the inferior surface of the vertebral body along a line posterior point to anterior point of vertebral body and positive forward. The z-axis is positive downward. For C1, two inferior points, represented as red dots in Fig. 6, were used to create the lower vertebral coordinate for the occipital condyle. The initial angle of the x-axis defined on C7 was measured in the sled coordinate system and listed in Table II.

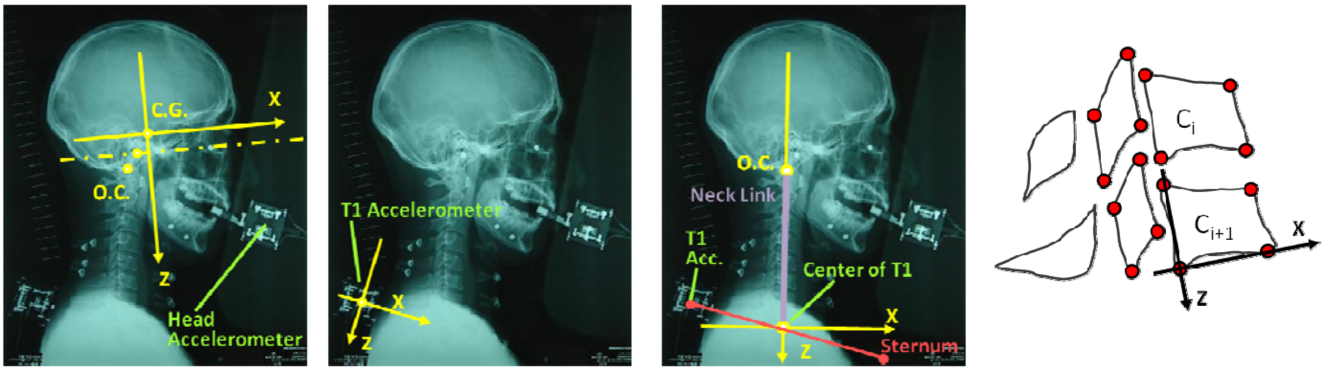

(a) Head anatomical coordinate system (b) T1 accelerometer coordinate system (c) T1 anatomical coordinate system (d) Lower vertebral coordinate system

Fig. 5. Definitions of four local coordinate systems. X-ray images were taken before testing in test series 2.

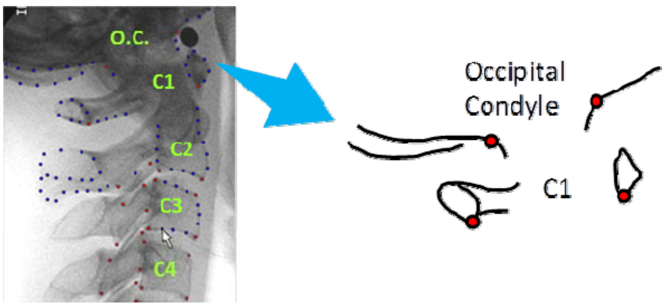

Fig. 6. Digitized points for the Occipital condyle and C1.

Analysis of Head and T1 Accelerations and Upper Neck Loads

The accelerometer data from the head rig in test series 1 and mouthpiece in test series 2 were transformed to the head c.g. in the head anatomical coordinate system as the head accelerations. Upper neck loads [16-17] at the occipital condyles were calculated based on the head accelerations and head mass properties, obtained from regression equations [18-20]. The T1 accelerometer data in the T1 accelerometer coordinate system were used in test series 1. For test series 2, the T1 accelerometer data were transformed to the centre of T1 in the T1 anatomical coordinate system.

Analysis of Whole Body Kinematics

The target markers attached to volunteers were tracked in the sled coordinate system and the estimated displacement of the head c.g., center of the occipital condyle, centre of T1 and pelvis were calculated in the sled coordinate system. For the center of the occipital condyle, positional relation relative to the target marker at the auditory canal was obtained from X-ray images shown in Fig. 5 and used in the calculation. The head c.g. displacement was also expressed in the T1 anatomical coordinate system.

The angular displacement of the head and T1 were extracted in the sled coordinate system from the high-speed video tracking. In order to analyze the head-neck kinematics, the line from the center of T1 to the center of the occipital condyles was defined as a purple line in Fig. 5 (c), hereafter referred to as the neck link, and the angular displacement of the line was calculated in the sled coordinate system. The angular displacements of the head relative to neck link and neck link relative to T1 rotation in the sled coordinate system were calculated.

Analysis of Cervical Spine Kinematics

In test series 2, four edge points of each vertebral body and the zygapophysial joint, represented as red dots in Fig. 5 (d), were digitized. The occipital condyle and C1 were digitized at two inferior points, represented as red dots in Fig. 6. For the translational displacement of the vertebrae, the midpoint between the two inferior points of each vertebral body was tracked. The vertebral angular displacements were calculated as the angle of a line connecting the two inferior points. All vertebral measurements were done in the coordinate system of the adjacent inferior vertebra, the lower vertebral coordinate system. Spline interpolation was applied to smooth the digitized raw data taken at a frame rate of 60 fps and plots were extracted at every 10ms. The total number of cineradiography images for one test was around 15-20 with 16.67 ms intervals. The resolution of cineradiography images was 1280 x 1024 pixels (approximately 7.3 pixels/mm). The mean errors of the digitized data on the inter-observer variations were 0.7 deg in rotational angle, 0.44 mm in horizontal direction and 0.25 mm in vertical direction.

III. RESULTS

Fig. 7 and Fig. 8 show sequential images taken with a high-speed video camera in the two test series. The average time histories of the head c.g., T1 and pelvis displacement in the sled coordinate system are shown with corridors in the Appendix. Fig. 9 shows sequential images taken with cineradiography in test series 2. The cervical spine motions were tracked using these images. The average time histories of vertebra displacement and rotational angle with corridors in the lower vertebra coordinate system are shown in the Appendix. The time histories of the head c.g., T1 accelerations and neck loads are also shown in the Appendix. Time zero for all the data was defined as the time where the sled acceleration began to rise. The corridors were defined as the average ± one standard deviation (SD) from the average. Table III shows symptoms of the volunteers after the experiment in test series 2. 3 of 4 male volunteers complained about muscular pain and discomfort, fairly mild symptoms which disappeared within 3 days.

0ms 50ms 100ms 150ms 200ms 250ms

Fig. 7. Sequential high-speed video images (500 f/s) in test series 1, female volunteer (top row) and male volunteer from Ono [12](bottom row)

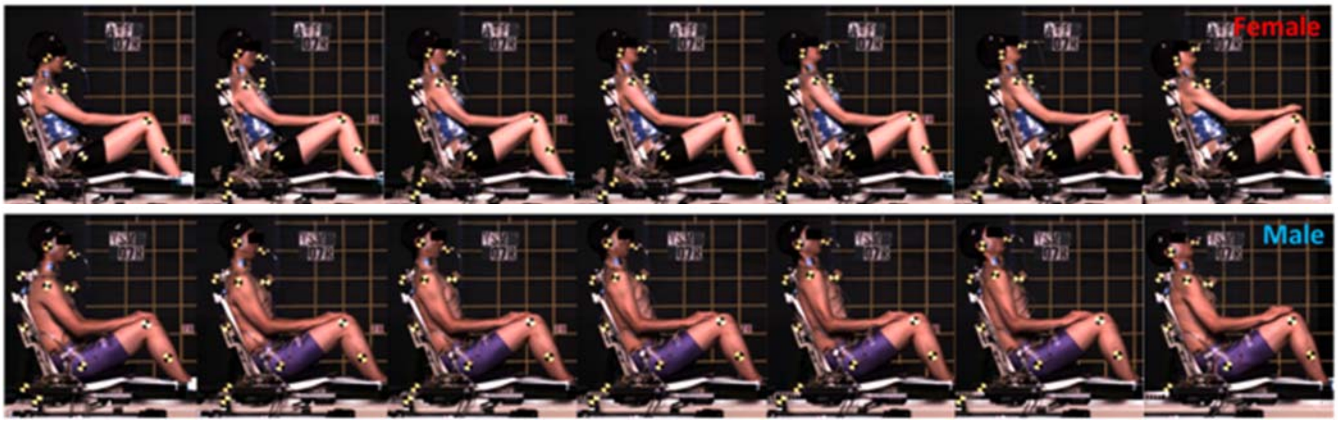

0ms 84ms 100ms 116ms 134ms 150ms 200ms

Fig. 8. Sequential high-speed video camera images (500 f/s) in test series 2, female volunteer (top row) and male volunteer (bottom row).

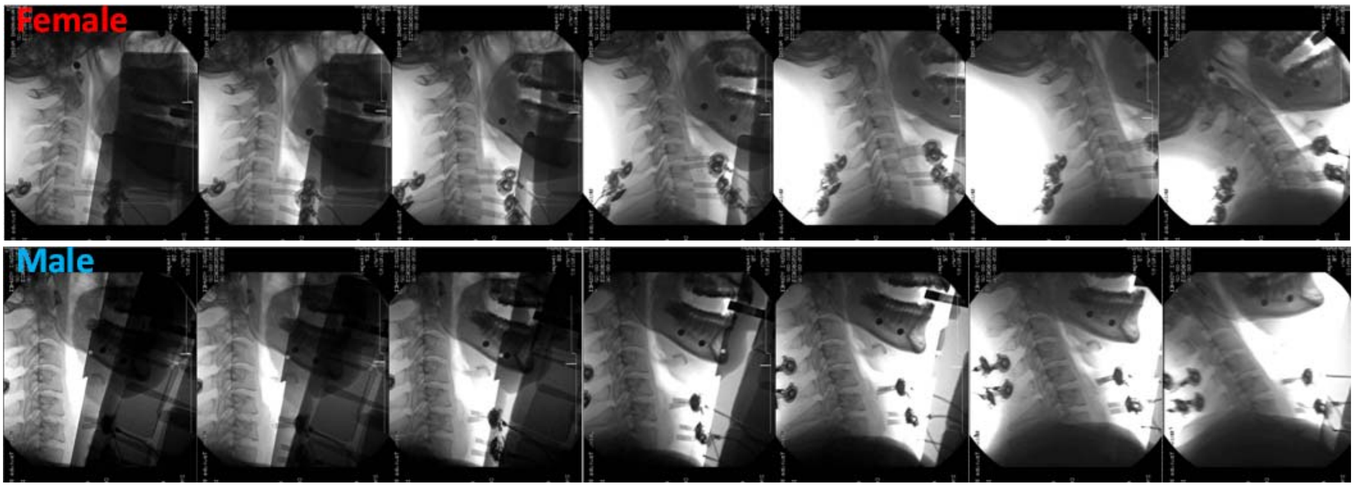

0ms 83ms 100ms 117ms 133ms 150ms 200ms

Fig. 9. Sequential cineradiography images (60 f/s) in test series 2, female volunteer (top row) and male volunteer (bottom row). The volunteers shown in these cineradiography images are the same subjects as those in Fig. 8.

TABLE III SYMPTOMS OF THE VOLUNTEERS AFTER THE EXPERIMENT IN TEST SERIES 2

ID	Sex	Symptoms after experiments
I	F	No symptom
II	F	No symptom
III	M	Neck muscular pain for 2 days
IV	M	Shoulder discomfort for 2 days
V	M	No Symptom
VI	M	Shoulder muscular pain only on that day

Head, Neck and T1 Kinematics

Fig. 10 (a) and Fig. 11 (a) show a gender comparison of the average time histories of the head and T1 angular displacement in the sled coordinate system in test series 1 and 2. The T1 angular displacement of females and males were similar. However, the head angular displacement was greater for females than for males in both test series.

Fig. 10 (b) and Fig. 11 (b) show a gender comparison of the average time histories of the head angular displacement relative to T1 in test series 1 and 2. The females had a smaller and earlier peak of the flexion angle.

Fig. 10 (c) and Fig. 11 (c) show a gender comparison of the average time histories of the head angular displacement relative to the neck link and neck link angular displacement relative to T1 in test series 1 and 2. The females had a peak flexion of the head relative to neck link, while the neck link was extension at the time of peak head flexion. On the other hand, the males had flexion in both the head relative to neck link and neck link relative to T1 up to 100ms. Peaks appearing until 100 ms in test series 2 were observed clearly and are summarised in Fig. 12. At the end of the test series, both females and males exhibited extension.

Fig. 13 and Fig. 14 show a gender comparison of the average time histories and trajectories of the head displacement in the T1 coordinate system in the test series 1 and 2. The rearward displacement (negative X-direction) of the head relative to T1 was larger for the females than males at the time of peak head extension. The z displacement had a similar trend for the females and males until around 150ms.

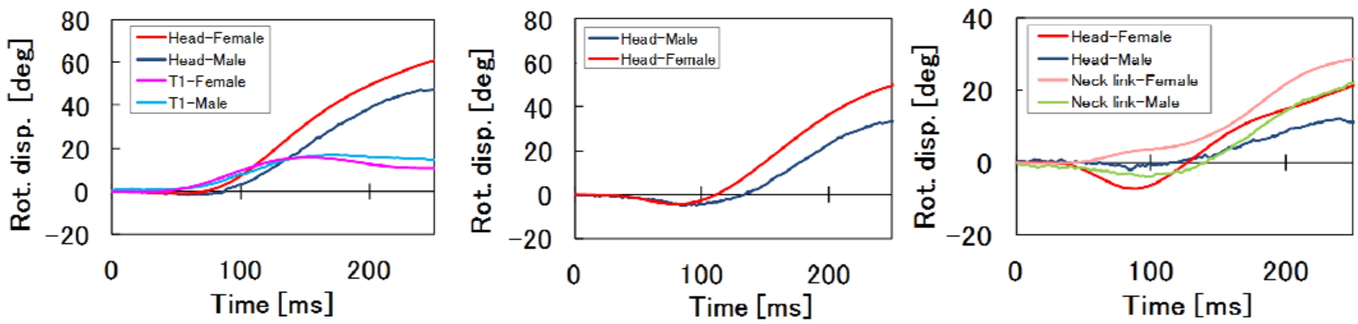

(a) Head and T1 angular displacement in the sled coordinate system

(b) Head angular displacement relative to T1

(c) Head angular displacement relative to neck link, and neck link angular displacement relative to T1

Fig. 10. Average time histories of the head, neck link and T1 angular displacement with sled pulse 1 in test series 1. The positive side is extension and negative flexion. The corridors defined as the average± SD are shown in Appendix.

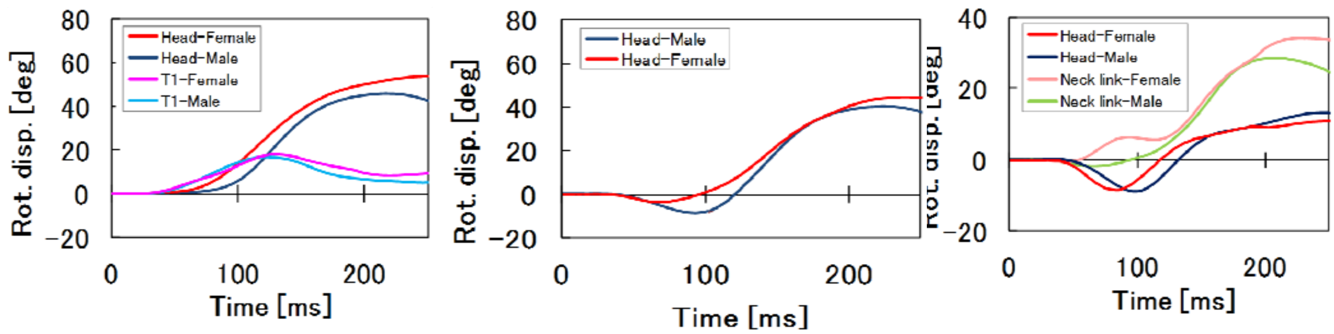

(a) Head and T1 angular displacement in the sled coordinate system

(b) Head angular displacement relative to T1

(c) Head angular displacement relative to neck link, and neck link angular displacement relative to T1

Fig. 11. Average time histories of the head, neck link and T1 angular displacement in test series 2. The positive side is extension and negative flexion. The corridors defined as the average± SD are shown in Appendix.

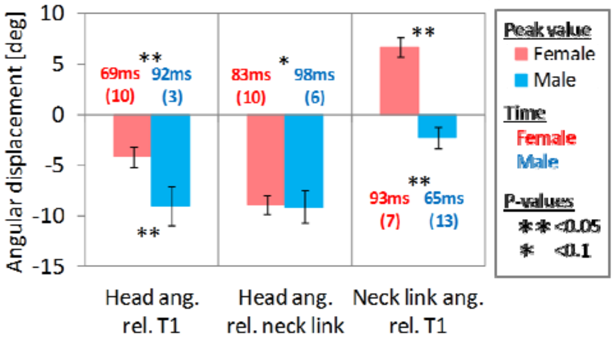

Fig. 12. The average angular displacement peaks and their timing for the head and neck link relative to T1 and head relative to neck link in test series 2. The average peak values in colored bars and standard deviation in black lines. The average timing in figures, standard deviation in parenthesis and p-values from t-test. The positive value is extension and negative flexion.

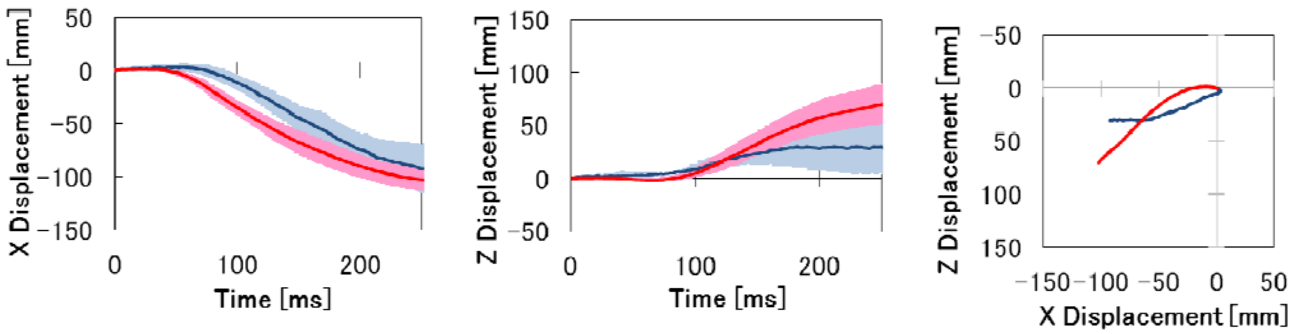

Fig. 13. Average time histories and trajectory of the head X and Z displacement in the T1 local coordinate for female (red) and male (blue) with sled pulse 1 in test series 1. The corridors were defined as the average ± one standard deviation from the average. The X displacement is positive forward and the z displacement positive downward.

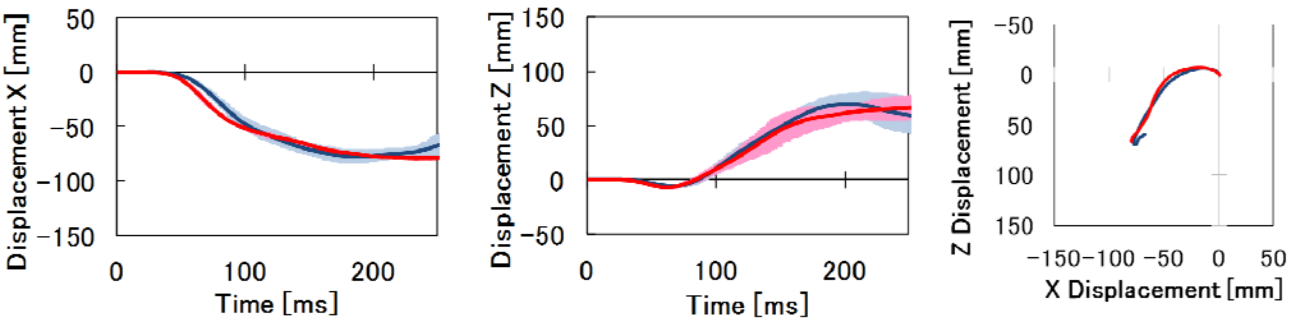

Fig. 14. Average time histories and trajectory of the head X and Z displacement in the T1 local coordinate for female (red) and male (blue) in test series 2. The corridors were defined as the average ± one standard deviation from the average. The X displacement is positive forward and the z displacement positive downward.

Vertebra kinematics in Cervical Spine Motion Analysis

Fig. 15 shows the average time histories of the vertebral angular displacement for female and male. The vertebral rotation varied between spinal segments, with larger differences between segments for the females compared to the males. C1/C2 exhibited the greatest average peak flexion angle of -8.1 degrees at 90ms for the female, -6.6 degrees at 100ms for the male average. At that point in time, the cervical spine was exposed to an S shape, with OC/C1, C1/C2 and C2/C3 in flexion and C4/C5, C5/C6 and C6/C7 in extension. C3/C4 was in flexion for the males and around neutral for the females. Fig. 16 shows a gender comparison of the vertebral angular displacement relative to the inferior vertebra at sampling times around the peak S shape. The lower neck extension was remarkably larger for the females than the males at 90 ms, giving the female necks a more pronounced S shape. Also, the flexion of the upper cervical spine seemed to start earlier for the females than the males and have slightly higher values, especially at the C1/C2 level. The cervical spine responses observed in this study corresponded to a previous study reported by Stemper [9] with post mortem human head-neck complexes.

Fig. 17 shows the average time histories of the vertebral displacement in X-direction normalised by the length of the inferior surface of the vertebral body. Fig. 18 shows a gender comparison of the normalised vertebral displacement in X-direction at sampling times around the peak S shape. The vertebral displacement in X-direction varied between spinal segments, with larger differences between segments for the females compared to the males. The upper neck at C1/C2 and the lower neck at C4/C5 to C6/C7 exhibited rearward displacement. C3/C4 showed virtually no displacement around the peak S shape.

Fig. 19 shows the average time histories of the vertebral displacement in Z-direction normalised by the length of the inferior surface of the vertebral body in the lower vertebra coordinate system. Fig. 20 shows a gender comparison of the normalised vertebral displacement in Z-direction at sampling times around the peak S shape. C1/C2 exhibited the greatest peak upward displacement of -0.095 at 100ms for the female average and -0.110 at 100ms for the male average.

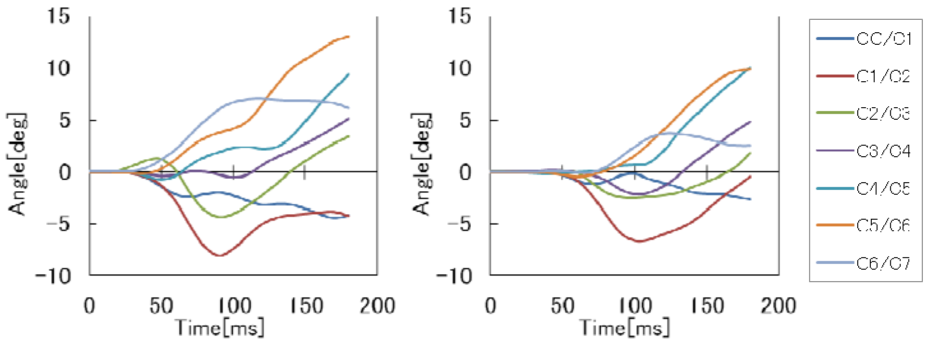

(a) Female (b) Male

Fig. 15. Time histories of the average of vertebral angular displacement relative to the inferior vertebra in the test series 2. The positive side is extension and negative flexion.

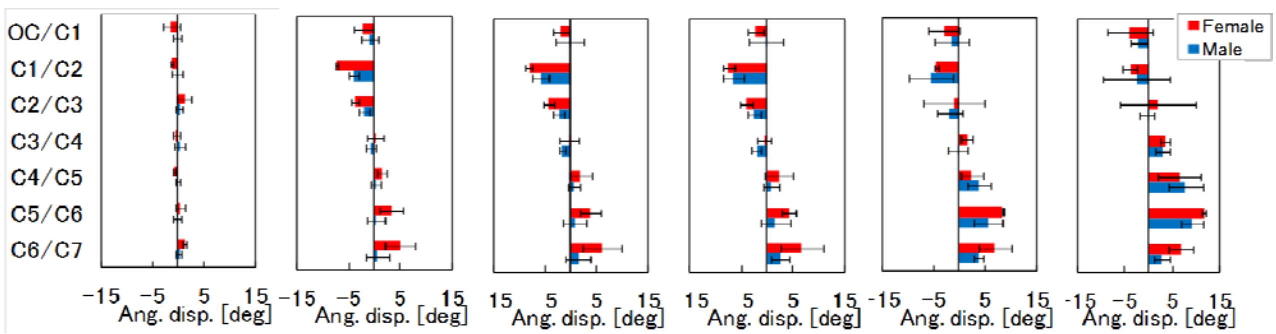

50ms 80ms 90ms 100ms 130ms 160ms

Fig. 16. The vertebral angular displacement relative to the inferior vertebra for female (red) and male (blue) in test series 2. Average in colored bars and standard deviation in black lines. The positive side is extension and negative flexion.

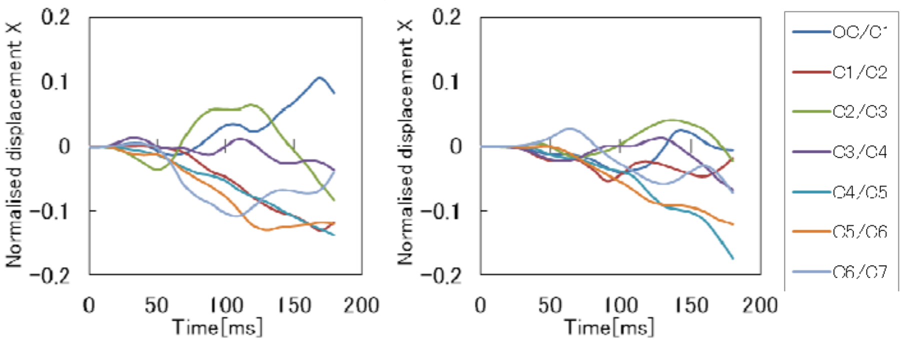

(a) Female (b) Male

Fig. 17. Time histories of the average of vertebral normalised displacement in X-direction in the lower vertebra coordinate system in test series 2. The positive side is forward and negative rearward.

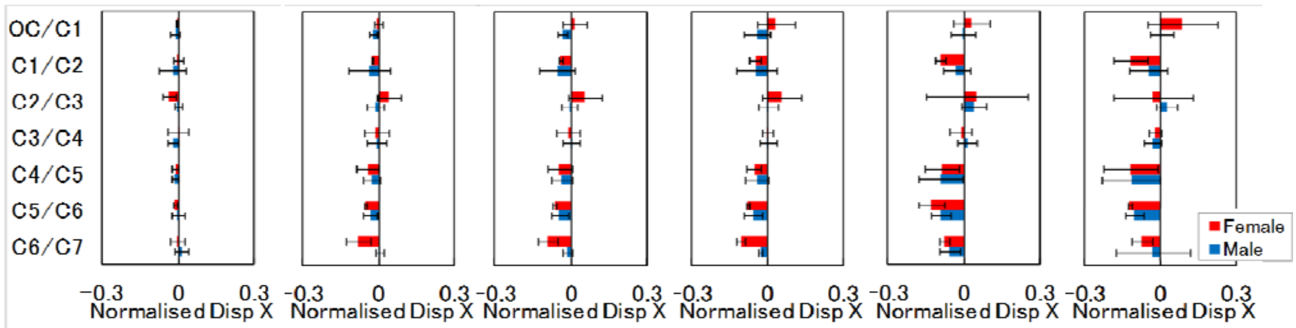

50ms 80ms 90ms 100ms 130ms 160ms

Fig. 18. The vertebral normalised displacement in X-direction in the lower vertebra coordinate system for female (red) and male (blue) in test series 2. Average in colored bars and standard deviation in black lines. The positive side is forward and negative rearward.

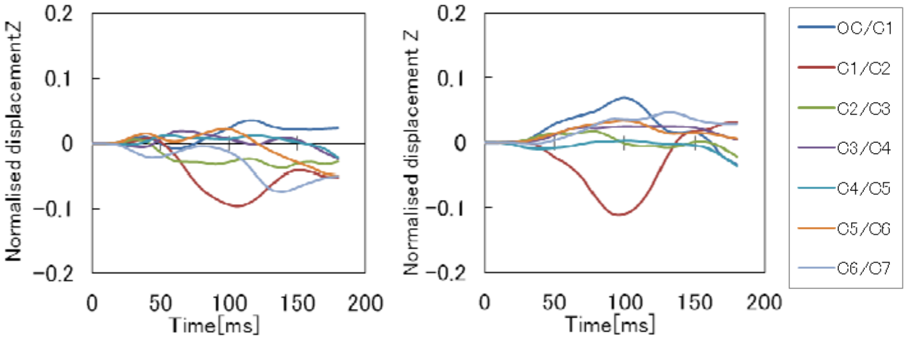

(a) Female (b) Male

Fig. 19. Time histories of the average of vertebral normalised displacement in Z-direction in the lower vertebra coordinate system in test series 2. The positive side is extension and negative flexion.

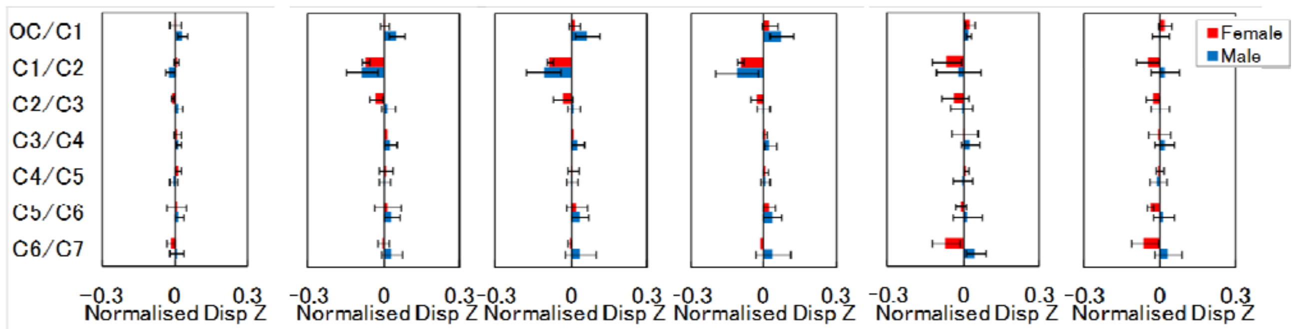

50ms 80ms 90ms 100ms 130ms 160ms

Fig. 20. The vertebral normalised displacement in Z-direction in the lower vertebra coordinate system for female (red) and male (blue) in test series 2. Average in colored bars and standard deviation in black lines. The positive side is downward and negative upward.

IV. DISCUSSION

In the overall motion analysis, the head and T1 rotated in extension in the sled coordinate system. Initially the head rotated in flexion relative to T1 and later switched to extension for both genders in both test series. The females had a greater extension angle of the head relative to T1 compared to the males at the end of the test, but the initial peak flexion angle was smaller for the females compared to the males. This phenomenon of the initial flexion seemed to affect the males' neck deformation more than the females. However, Fig. 10 (c) and Fig. 11 (c) showed that only the females' neck link rotated in extension relative to T1 at the time of the peak head flexion, and the difference between the head angle relative to neck link and neck link relative to T1 was larger for the females compared to the males. Likewise, the females had larger flexion in the upper vertebral segments and larger extension in lower vertebral segments, when analysing the cervical spine motion. Thus, the difference between the upper and lower vertebral rotation was larger for the females compared to the males and the females were exposed to more pronounced S-shape deformation of the neck. The cineradiography data showed the same tendency as that of the overall motion analysis and supported that the head relative to neck link and neck link relative to T1 indicated S-shape deformation of the neck.

Carlsson [5] analysed a rear impact test series with 11 male and 12 female volunteers [8] at the same impact level as this study. The study reported that head-to-head restraint contact time was 91ms for females and 100ms for males at a ΔV of 8km/h. Pramudita [14] also conducted a rear impact test series with 6 male and 3 female volunteers at the same impact level as this study, and reported that head-to-head restraint contact time was 95ms for males with the maximum sled acceleration of $40m/s^2$. In this study the cervical S-shape motion was observed around those head-to-head restraint contact timings. Therefore, the female volunteers in those studies had possibilities to be exposed to more pronounced S-shape deformation of the neck than the males before head-to-head restraint contact.

Previous studies have investigated the prevalence of neck pain at the cervical zygapophysial joint in rear-end impacts and reported that the majority of patients experienced chronic pain at either C2/C3 [21] or C5/C6 [21-23]. The study of a rear impact test series with cadavers [24] reported that small damages were found at C5/C6 and C6/C7 level at autopsy. In this study, C2/C3 showed most forward displacement for the females in the upper neck region and C5/C6 exhibited the largest angular and translational displacements at the time around the peak S shape, especially for the females.

Limitations

The cineradiography data were taken with only 2 female and 4 male volunteers. It was insufficient to generalise female and male characteristics of cervical vertebral motion; therefore, this study was complemented with the overall head, neck and thorax kinematics in test series 1. However, the cineradiography data are valuable and significant in revealing dynamic cervical vertebral kinematics and understanding the local deformation of the spinal segments. Furthermore, since the tests were conducted using an experimental rigid seat without head restraint, it is difficult to predict the cervical motion using a commercial vehicle seat with head restraint.

V. CONCLUSIONS

This study investigated the characteristics of dynamic head, neck and torso (T1) kinematics and individual cervical vertebral motion for both females and males by analysing volunteer responses from two series of rear impact sled tests. The following most important findings were obtained:

- T1 angular displacements for females and males were of the same magnitude, while the head angular displacement was larger for females than for males.
- Females had a smaller and earlier peak flexion of the head angular displacement relative to T1.
- Females had a peak flexion of the head relative to neck link, while the neck link was extension at the time of peak head flexion. On the other hand, the males had flexion in both the head relative to neck link and neck link relative to T1 up to 100ms.
- The rearward displacement of the head relative to T1 was larger for females than males around the timing of the initial peak head angular displacement.
- The vertebral angular displacements were larger for females than males for all spinal segments during almost the whole sled test duration.
- C1/C2 exhibited the greatest peak flexion. At that point in time, OC/C1 to C2/C3 was in flexion and C4/C5 to C6/C7 in extension. C3/C4 for the males was also in flexion and for females around neutral.
- The upper neck at C1/C2 and lower neck at C4/C5 to C6/C7 exhibited rearward displacement. C3/C4 showed virtually no displacement around the peak S shape.
- C1/C2 exhibited the greatest peak upward displacement for both genders.

VI. REFERENCES

[1] Watanabe Y, Ichikawa H, Kayama O, Ono K, Kaneoka K, Inami S. Influence of seat characteristics on occupant motion in low-velocity rear-end impacts, *Accident Analysis and Prevention*, 2000, 32:243-250.

[2] Krafft M. When do AIS 1 neck injuries result in long-term consequences - Vehicle and Human Factors, *Traffic Injury Prevention*, 2002, 3(2):89-97.

[3] Kullgren A, Krafft M. Gender analysis on whiplash seat effectiveness: results from real-world crashes, *Proceedings of IRCOBI Conference,* 2010, Hanover, Germany.

[4] Kullgren A, Stigson H, Krafft M. Development of whiplash associated disorders for male and female car occcupants in cars launched since the 80s in different impact directions, *Proceedings of IRCOBI Conference, 2013, Göteborg*, Sweden.
[5] Carlsson A, Siegmund GP, Linder A, Svensson M. Motion of the head and neck of female and male volunteers in rear impact car-to-car tests at 4 and 8 km/h, *Proceedings of IRCOBI Conference*, 2010, Hanover, Germany.
[6] Harder S, Veilleus M, Suissa S. The effect of socio-demographic and crash-related factors on the prognosis of whiplash, *Journal of Clinical Epidemiology*, 1998, 51(5):377-384.
[7] Linder A, Carlsson A, Svensson MY, Siegmund GP. Dynamic responses of female and male volunteers in rear impacts, *Traffic Injury Prevention*, 2008, 9(6):592-599.
[8] Siegmund GP, King DJ, Lawrence JM, Wheeler JB, Brault JR, Smith TA. Head/neck kinematic response of human subjects in low-speed rear-end collisions, *Proceedings of 41th Stapp Car Crash Conference*, 1997, Lake Buena Vista, FL, USA, SAE paper 973341.
[9] Stemper BD, Yoganandan N, Pinter F. Gender dependent cervical spine segmental kinematics during whiplash*, Journal of Biomechanics*, 2003, 36(9):1281-1289.
[10] Matsushita T, Sato TB, Hirabayashi K, Fujimura S, Asazuma T, Takatori T. X-ray study of the human neck motion due to head inertia loading, *Proceedings of 38th Stapp Car Crash Conference*, 1994, Fort Lauderdale, FL, USA, SAE paper 942208.
[11] Ono K, Kaneoka K. Motion analysis of human cervical vertebrae during low speed rear impacts by the simulated sled, *Proceedings of IRCOBI Conference*, 1997, Hanover, Germany.
[12] Ono K, Inami S, et al. Relationship between localized spine deformation and cervical vertebral motions for low speed rear impacts using human volunteers, *Proceedings of IRCOBI Conference,* 1999, Sitges (Barcelona), Spain.
[13] Ono K, Ejima S, Suzuki S, Kaneoka K, Fukushima M, Ujihashi S. Prediction of neck injury risk based on the analysis of localized cervical vertebral motion of human volunteers during low-speed rear impacts, *Proceedings of IRCOBI Conference,* 2006, Madrid, Spain.
[14] Pramudita JA, Ono K, Ejima S, Kaneoka K, Shiina I, Ujihashi S. Head/neck/torso behavior and cervical vertebral motion of human volunteers during low speed rear impact: mini-sled tests with mass production car seat, *Proceedings of IRCOBI Conference,* 2007, Maastricht, The Netherlands.
[15] Beier G, Schuller E, Schuck M, Ewing CL, Becker ED, Thomas DJ. Center of gravity and moments of inertia of human heads, *Proceedings of IRCOBI Conference*, 1980, Birmingham, England.
[16] Mertz HJ, Patrick LM. Investigation of the kinematics and kinetics of whiplash, *Proceedings of 11th Stapp Car Crash Conference*, 1967, Anaheim, CA, USA, SAE paper 670919.
[17] Ono K, Kanno M. Influences of the physical parameters on the risk to neck injuries in low impact speed rear-end collisions, *Proceedings of IRCOBI Conference,* 1993, Eindhoven, The Netherlands.
[18] Walker LB, Harris EH, Pontius UR. Mass, volume, centre of mass, and mass moment of inertia of head and head and neck of human body. *Proceedings of 17th Stapp Car Crash Conference*, 1973, Oklahoma City, Oklahoma, USA, SAE paper 730985.
[19] Ae M, Tang H, Yokoi T. Estimation of inertia properties of the body segments in Japanese athletes, Society of *Biomechanisms Japan*, 1992, 11:23-33.
[20] Yoganandan N, Pintar FA, Zhang J, Baisden JL. Physical Properties of the human head: Mass, center of gravity and moment of inertia, *Journal of Biomechanics*, 2009, 42:1177-1192.
[21] Barnsley L, Lord SM, Wallis BJ, Bogduk N. The prevalence of chronic cervical zygapophysial joint pain after whiplash, *Spine,* 1995, 20(1):20-25.
[22] Lord SM, Barnsley L, Wallis BJ, McDonald GJ, Bogduk N. Precutaneous radiofrequency neurotomy for chronic cervical zygapophysial joint pain, *New England Journal of Medicine*, 1996, 335(23):1721-1726.
[23] Liliang PC, Lu K, Hsieh C-H, Kao CY, Wang KW, Chen HJ. Pulsed radiofrequency of cervical medial branches for treatment of whiplash-related cervical zygapophysial joint pain*,* 2008, *Surgical Neurology*, 70(Supp1):50-55.
[24] White NA, Begeman PC, et al. Investigation of upper body and cervical spine kinematics of post mortem human subjects (PMHS) during low-speed, rear-end impacts, 2009, SAE paper 2009-01-0387.

VII. APPENDIX

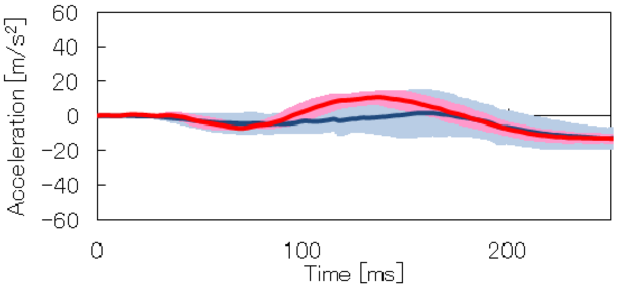

(a) Head c.g. X acceleration

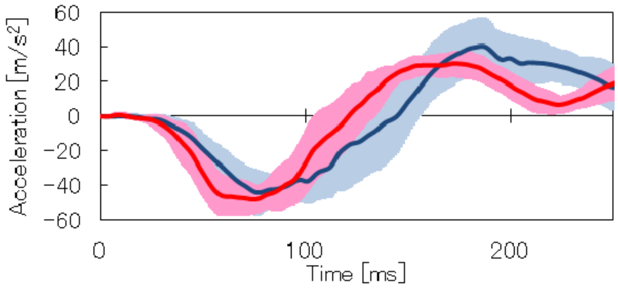

(b) Head c.g. Z acceleration

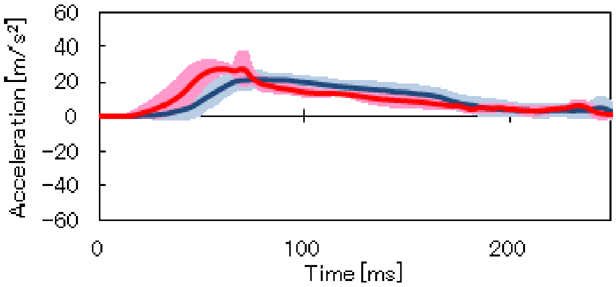

(c) T1 X acceleration

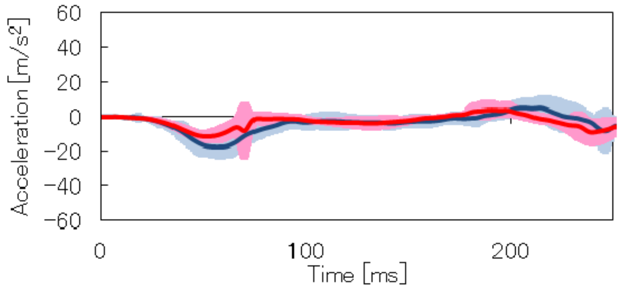

(d) T1 Z acceleration

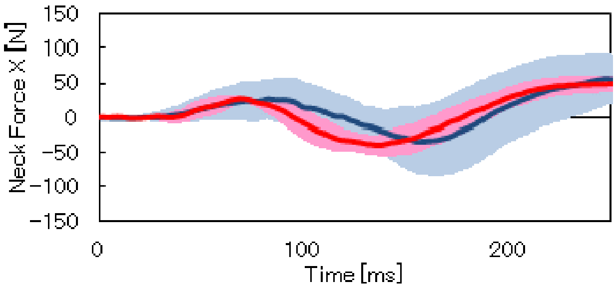

(e) Neck force X

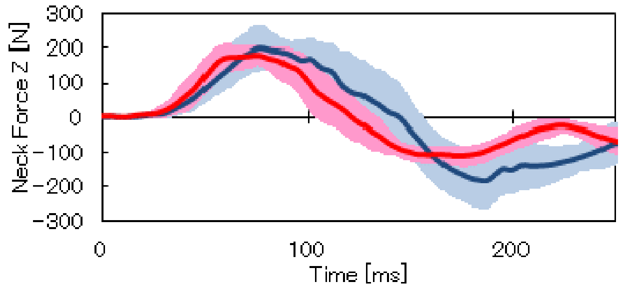

(f) Neck force Z

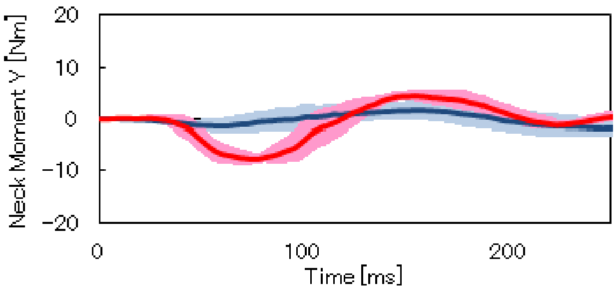

(g) Neck moment Y

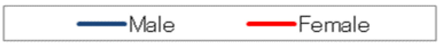

Fig. A1 Time histories of the average and corridor of accelerations and neck loads at the condition of sled pulse 1 in test series 1

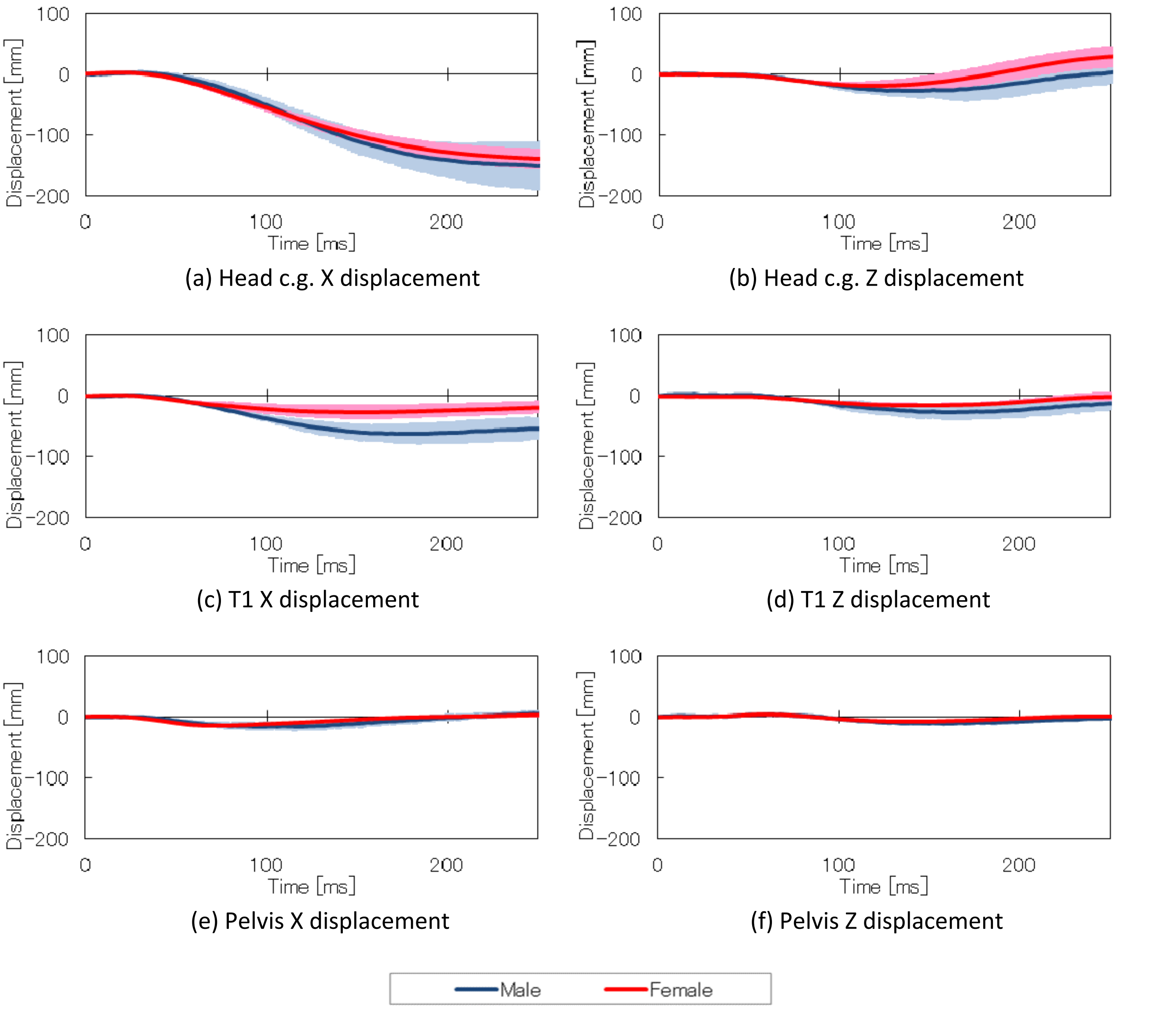

Fig. A2. Time histories of the average and corridor of displacements in the sled coordinate system at the condition of sled pulse 1 in test series 1

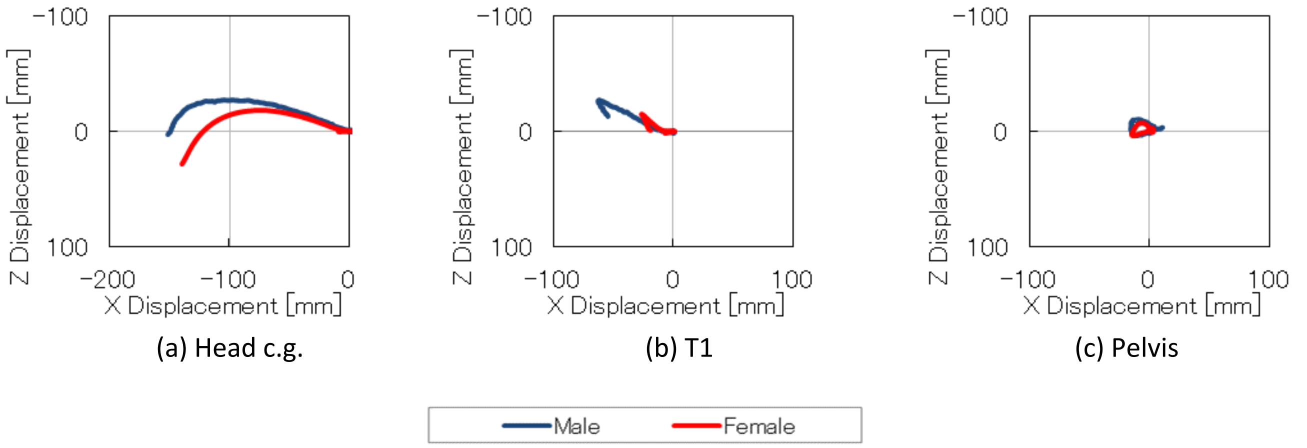

Fig. A3. Average displacements in XZ plane of the sled coordinate system at the condition of sled pulse 1 in test series 1

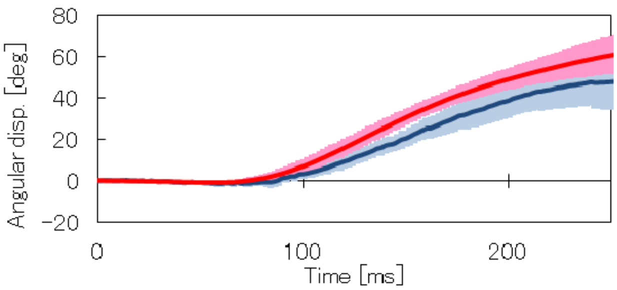

(a) Head Y angular displacement

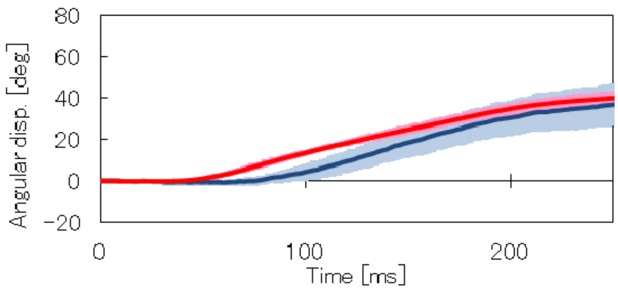

(b) Neck link Y angular displacement

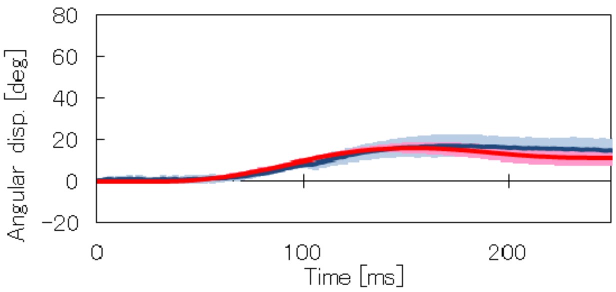

(c) T1 Y angular displacement

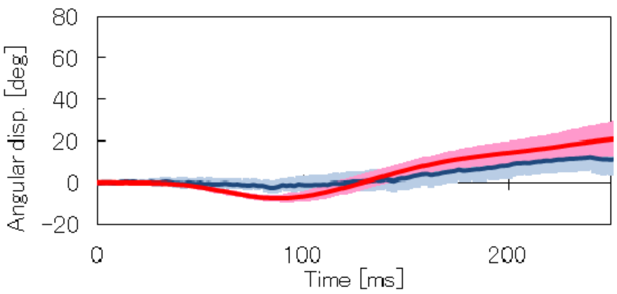

(d) Head Y angular displacement relative to neck link

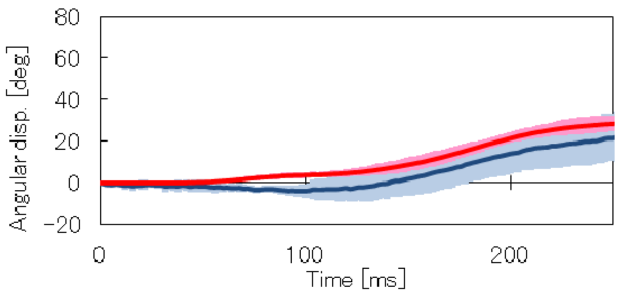

(e) Neck link Y angular displacement relative to T1

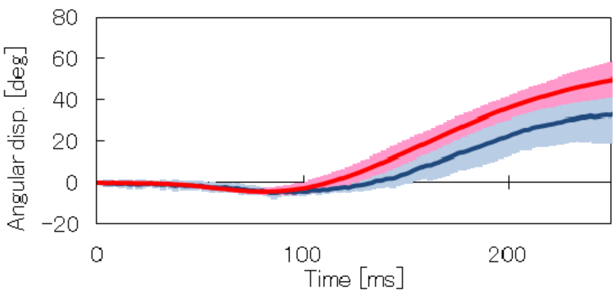

(f) Head Y angular displacement relative to T1

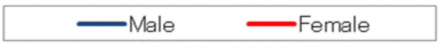

Fig. A4. Time histories of the average and corridor of angular displacements in the sled coordinate system at the condition of sled pulse 1 in test series 1

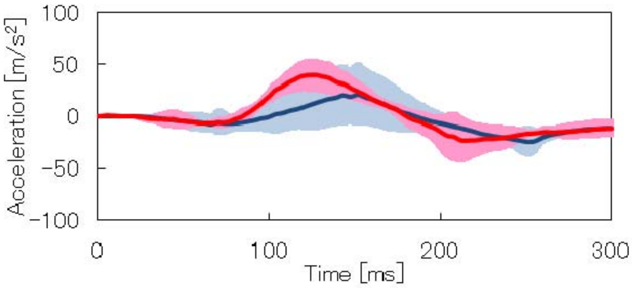

(a) Head c.g. X acceleration

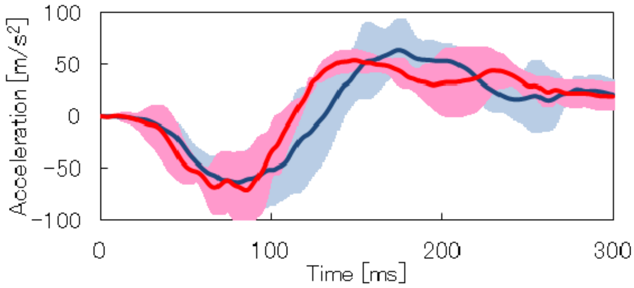

(b) Head c.g. Z acceleration

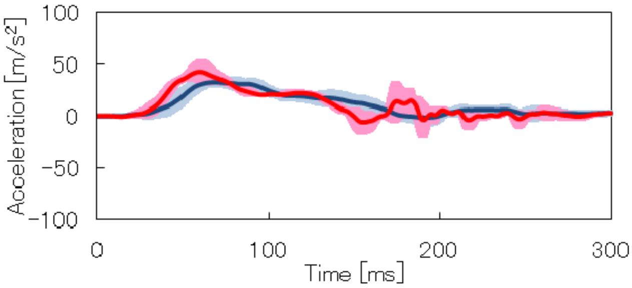

(c) T1 X acceleration

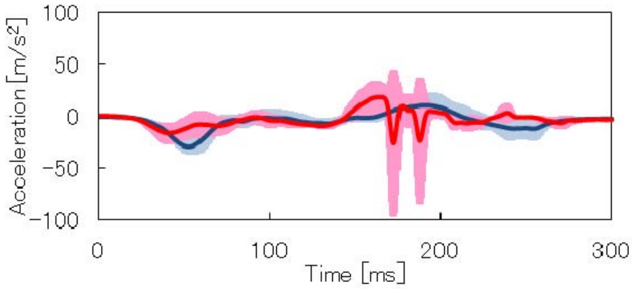

(d) T1 Z acceleration

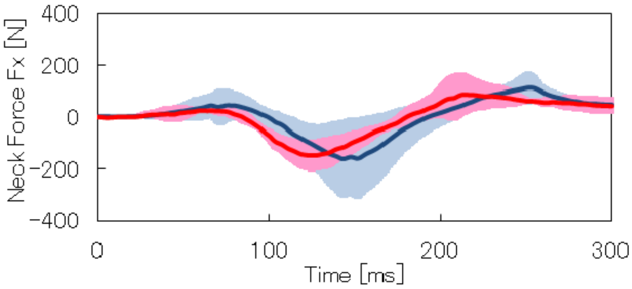

(e) Neck force X

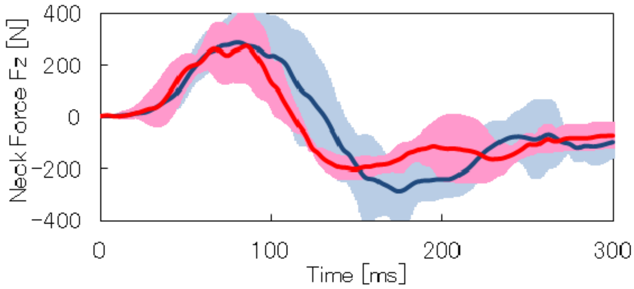

(f) Neck force Z

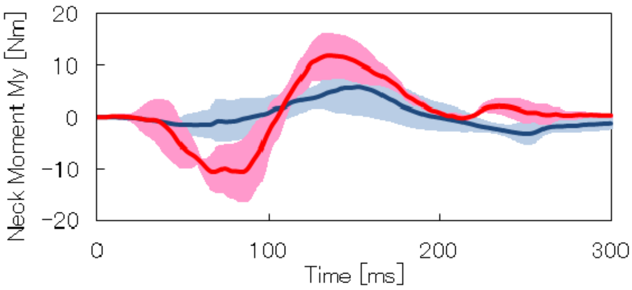

(g) Neck moment Y

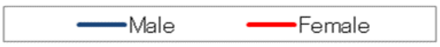

Fig. A5 Time histories of the average and corridor of accelerations and neck loads at the condition of sled pulse 2 in test series 1

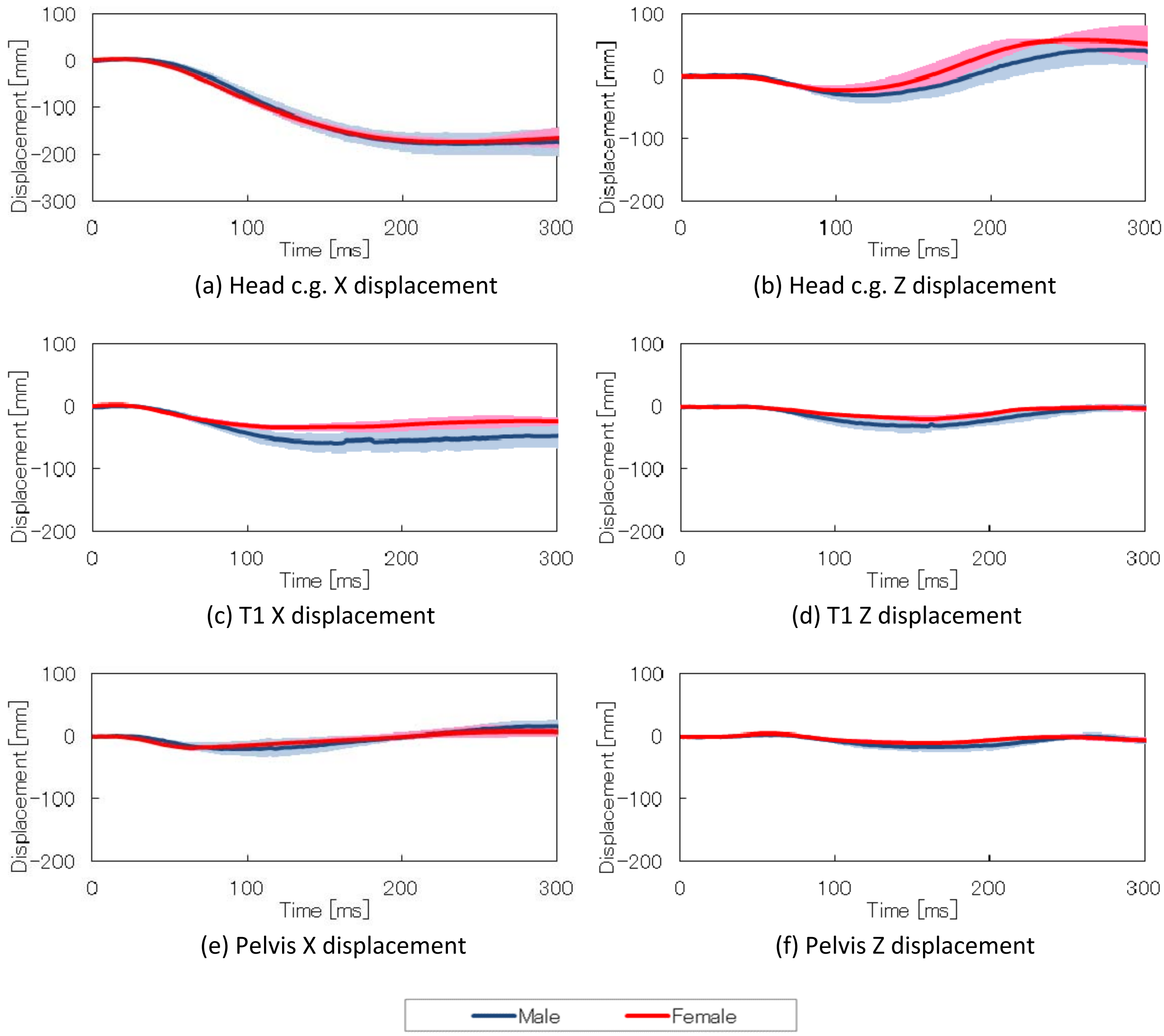

Fig. A6. Time histories of the average and corridor of displacements at the condition of sled pulse 2 in test series 1

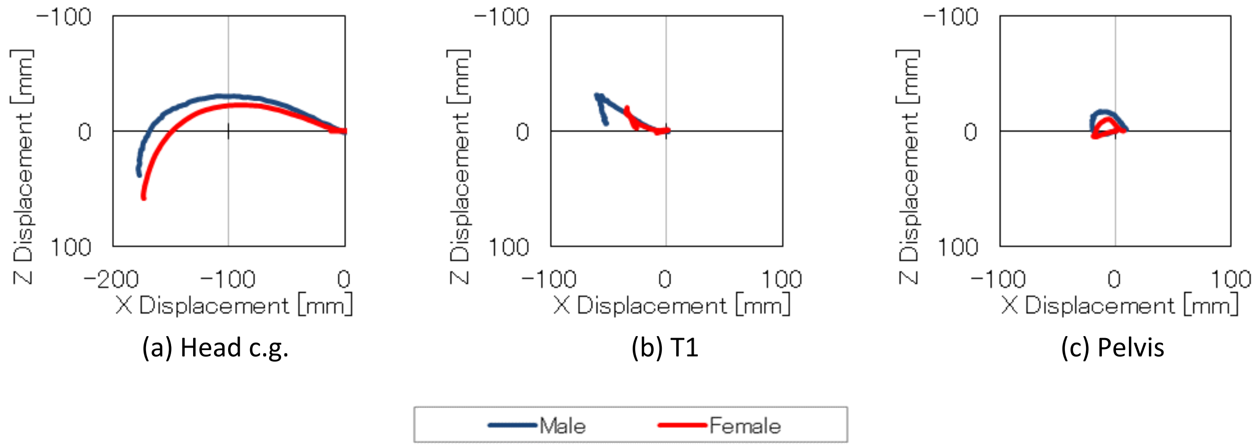

Fig. A7. Average displacements in XZ plane of the sled coordinate system at the condition of sled pulse 2 in test series 1

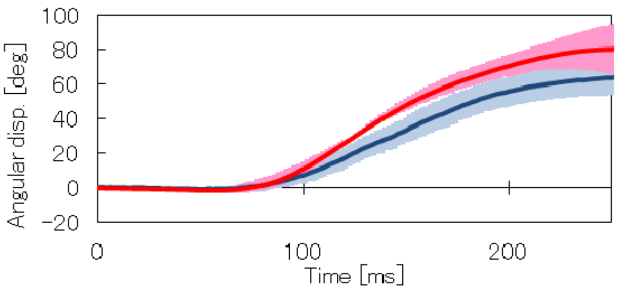

(a) Head Y angular displacement

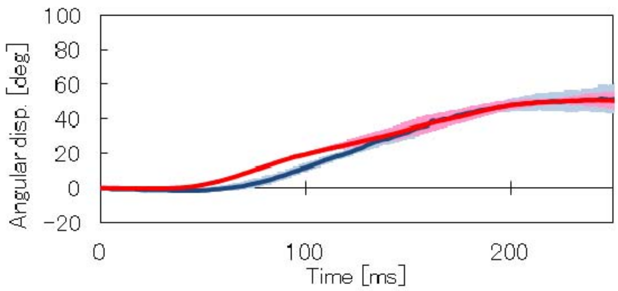

(b) Neck link Y angular displacement

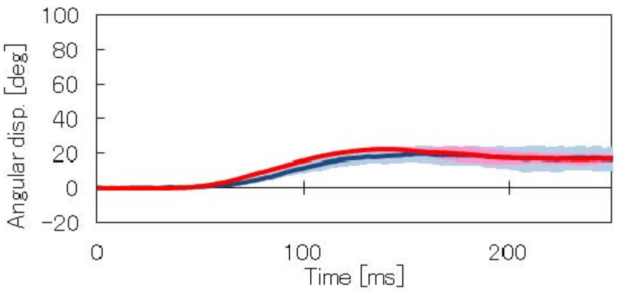

(c) T1 Y angular displacement

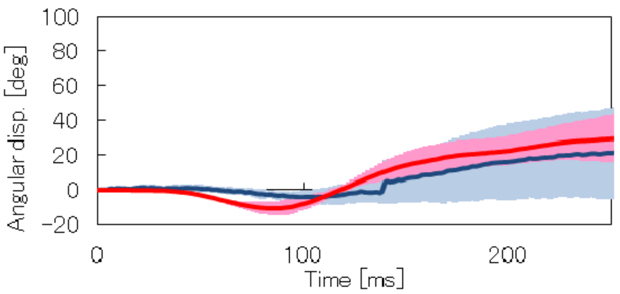

(d) Head Y angular displacement relative to neck link

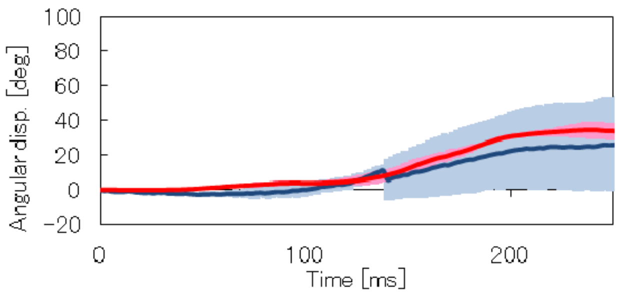

(e) Neck link Y angular displacement relative to T1

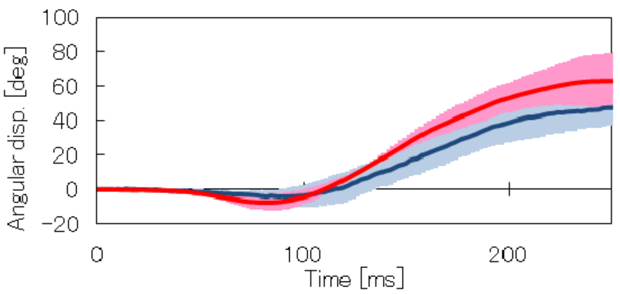

(f) Head Y angular displacement relative to T1

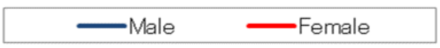

Fig. A8. Time histories of the average and corridor of angular displacements in the sled coordinate system at the condition of sled pulse 2 in test series 1

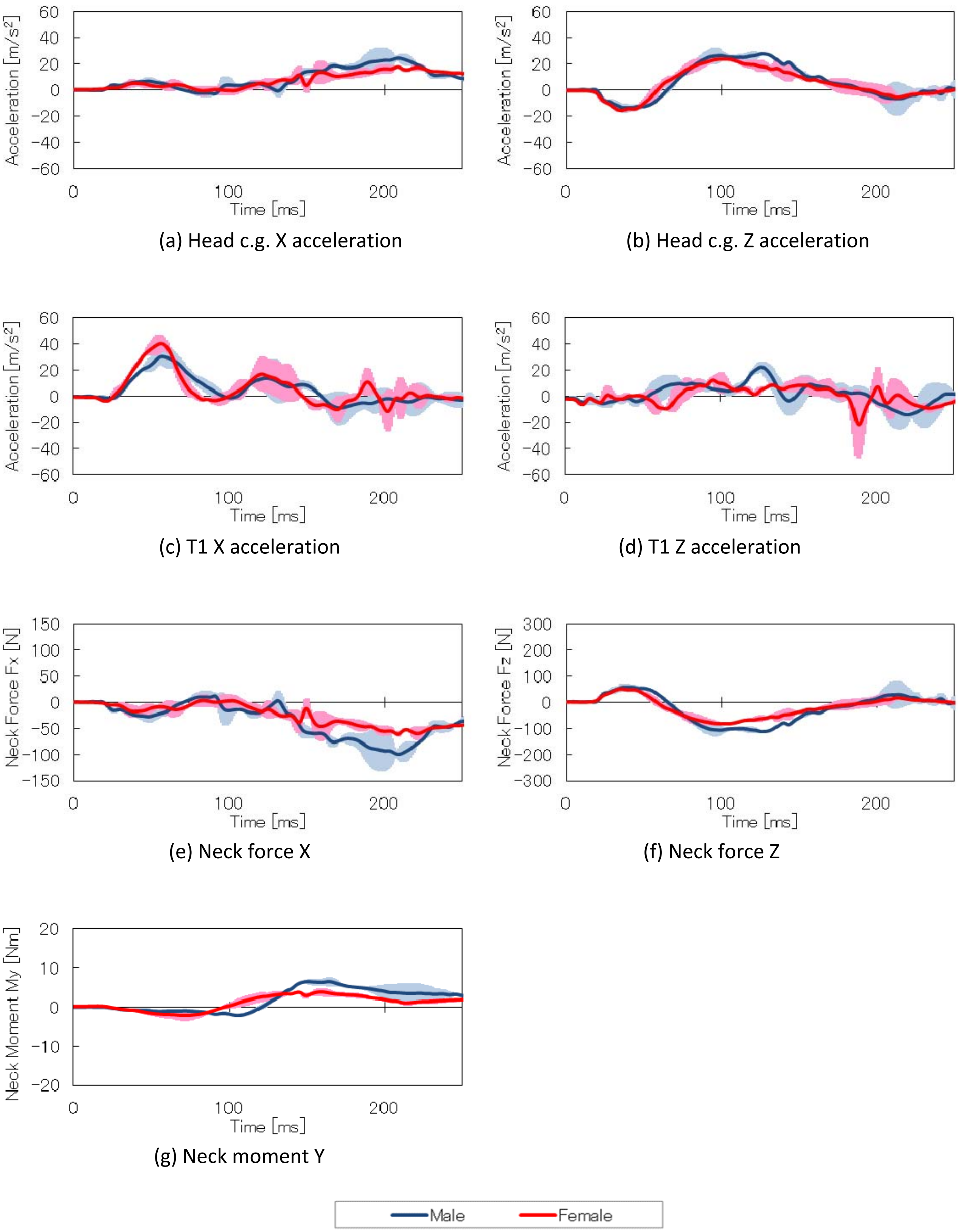

(a) Head c.g. X acceleration

(b) Head c.g. Z acceleration

(c) T1 X acceleration

(d) T1 Z acceleration

(e) Neck force X

(f) Neck force Z

(g) Neck moment Y

Fig. A9. Time histories of the average and corridor of accelerations and neck loads in test series 2

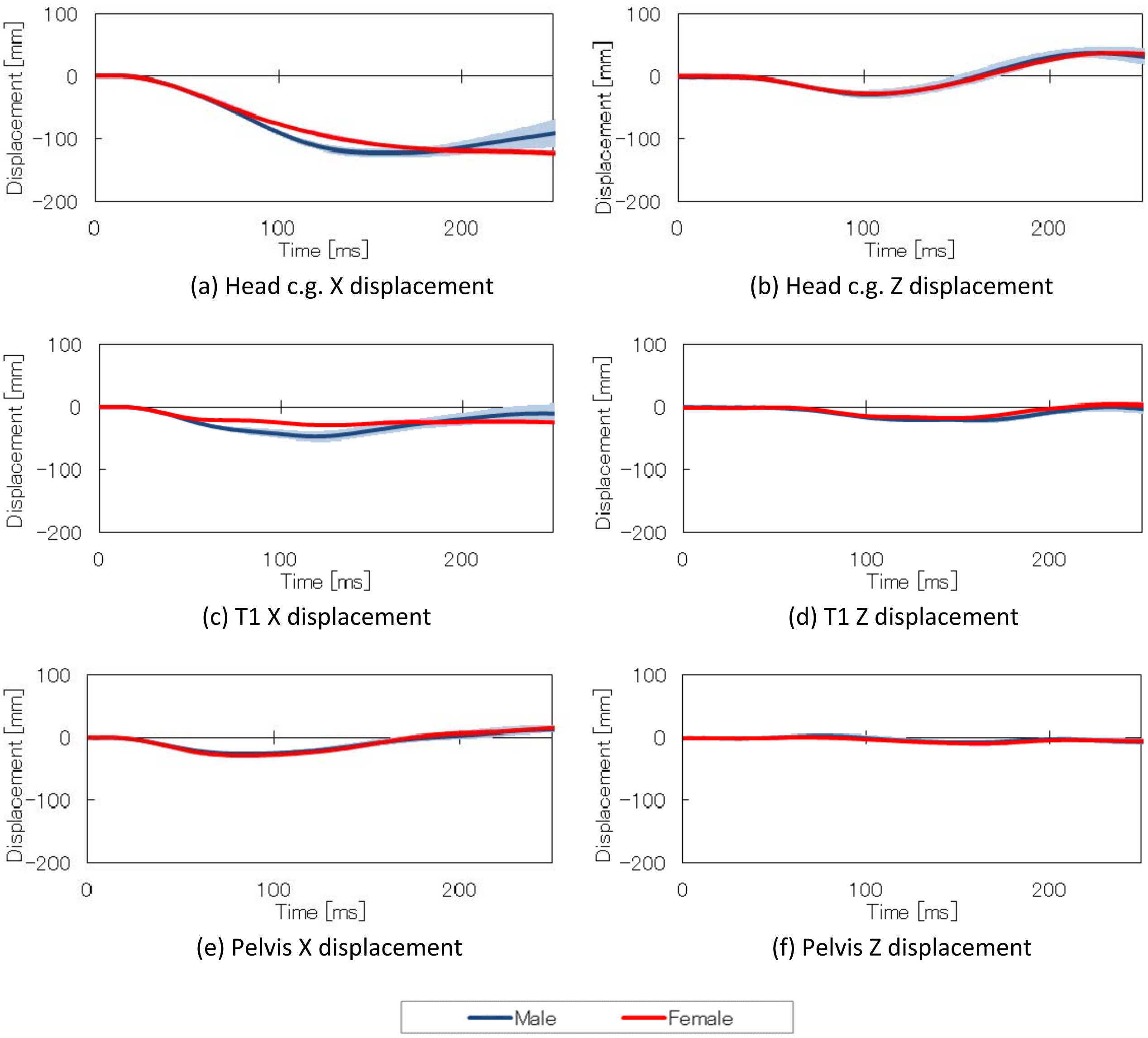

Fig. A10. Time histories of the average and corridor of displacements in test series 2

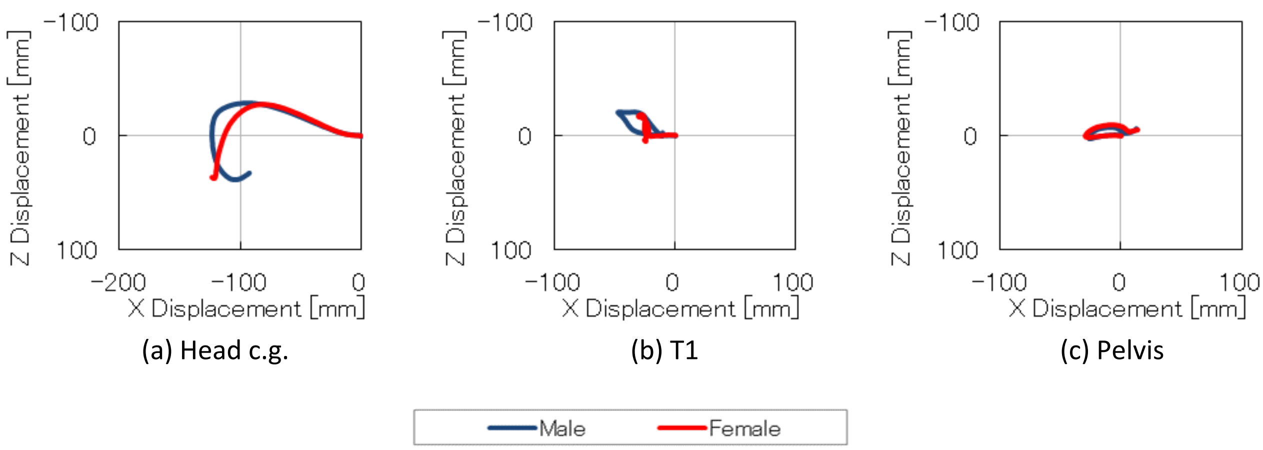

Fig. A11. Average displacements in XZ plane of the sled coordinate system in test series 2

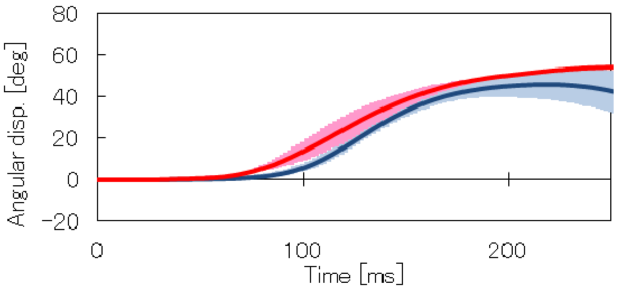

(g) Head Y angular displacement

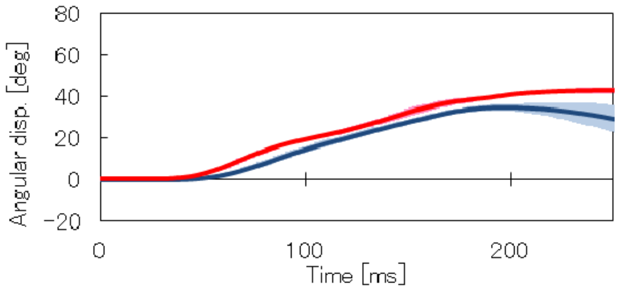

(h) Neck link Y angular displacement

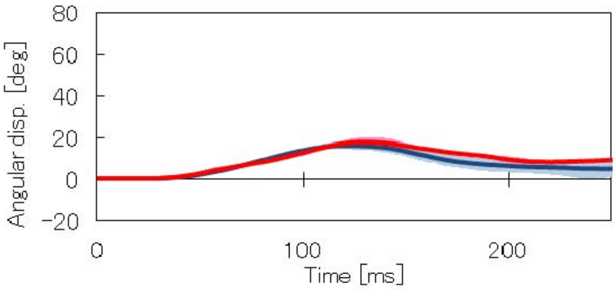

(i) T1 Y angular displacement

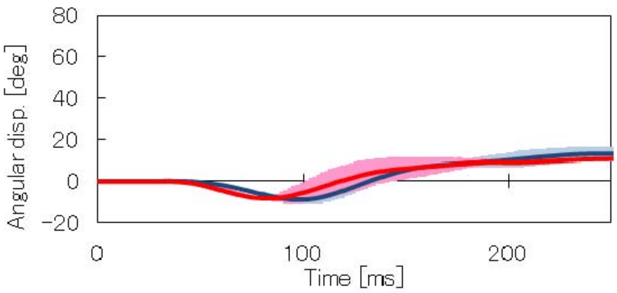

(d) Head Y angular displacement relative to neck link

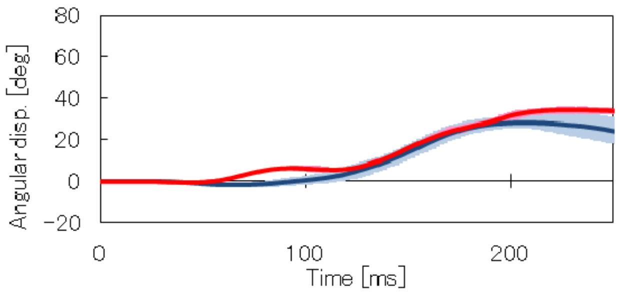

(e) Neck link Y angular displacement relative to T1

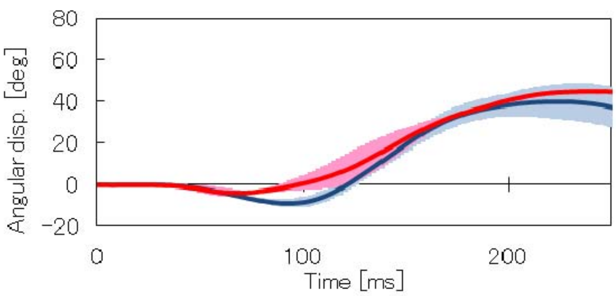

(f) Head Y angular displacement relative to T1

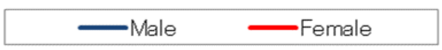

Fig. A12. Time histories of the average and corridor of displacements in test series 2

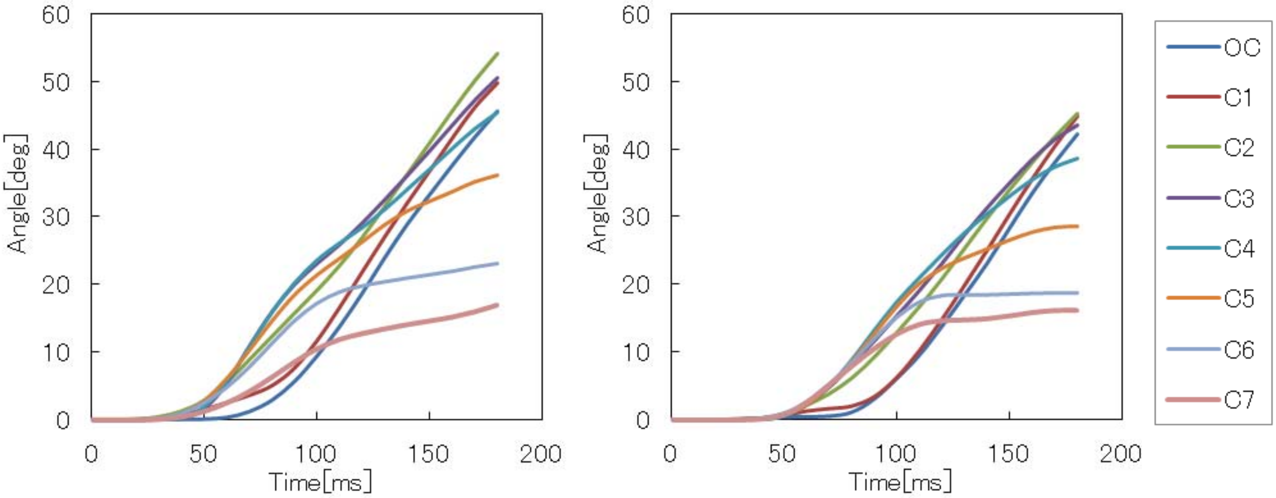

(a) Female (b) Male

Fig. A13. Time histories of the average of vertebral angular displacement in the sled coordinate system in test series 2

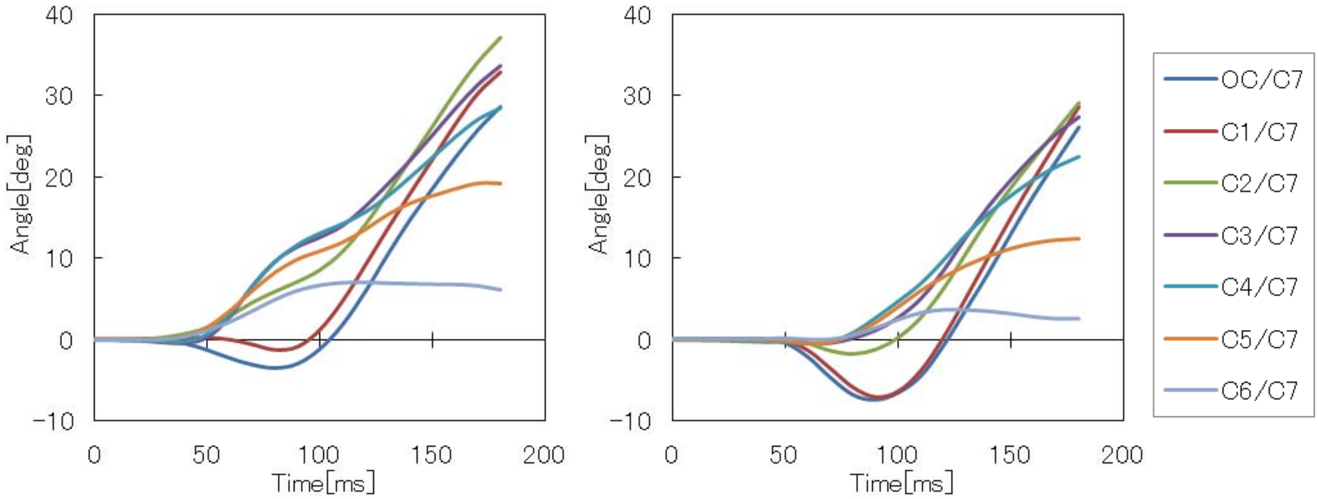

(a) Female (b) Male

Fig. A14. Time histories of the average of vertebral angular displacement relative to C7 in test series 2

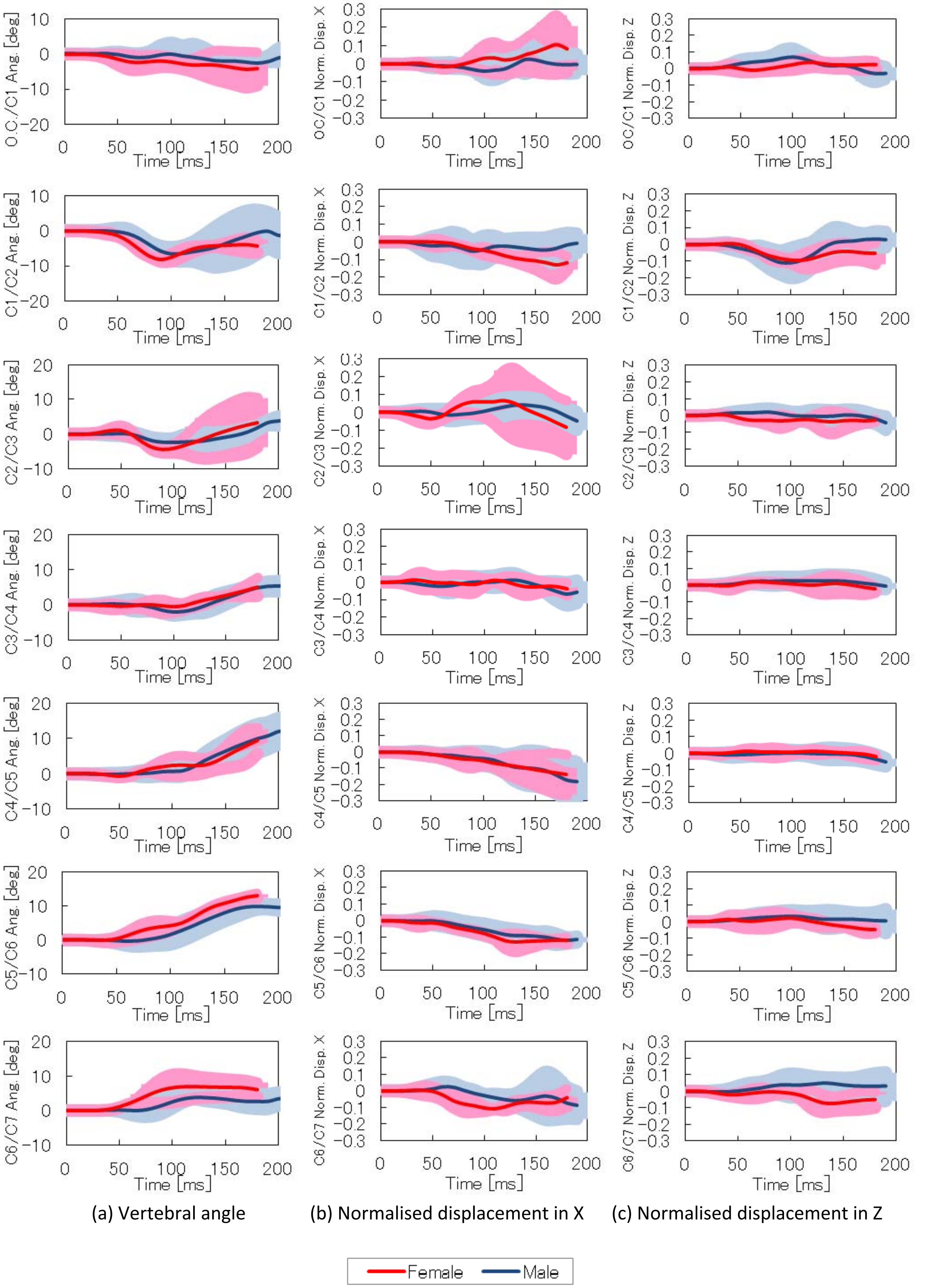

Fig. A15. Time histories of the average and corridor of vertebral angular and normalised displacements in the lower vertebra coordinate system in test series 2